Journal of Physics: Conference Series **659** (2015) 012027 doi:10.1088/1742-6596/659/1/012027

A Geometric Approach to Decouple Robotino Motions and its Functional Controllability

Daniel Straßberger, Paolo Mercorelli

Institute of Product and Process Innovation, Leuphana University of Lueneburg, Volgershall 1, D-21339 Lueneburg, Germany Phone: +49-(0)4131-677-5571, Fax: +49-(0)4131-677-5300.

E-mail: mercorelli@uni.leuphana.de

Oleg Sergiyenko

Engineering Institute of Autonomous University of Baja California, Blvd. Benito Juárez y Calle de La Normal, s/n, Col. Insurgentes Este, C.P.21280, Mexicali, BC, Mexico, tel./fax. 01(52-686) 566-41-50.

E-mail: srgnk@iing.mxl.uabc.mx

Abstract. This paper analyses a functional control of the Robotino. The proposed control strategy considers a functional decoupling control strategy realized using a geometric approach and the invertibility property of the DC-drives with which the Robotino is equipped. For a given control structure the functional controllability is proven for motion trajectories of class C^3, continuous functions with third derivative also being continuous. Horizontal, Vertical and Angular motions are considered and the decoupling between these motions is obtained. Control simulation results using real data of the Robotino are shown. The used control which enables to produce the presented results is a standard Linear Model Predictive Control (LMPC), even though for sake of brevity the standard algorithm is not shown.

1. Introduction

This paper presents a systematic procedure for obtaining the decoupling controllability between horizontal, vertical and angular motions and their functional controllability. Here in this contribution the functional decoupling problem is investigated and roughly speaking, it consists of achieving motion tracking with no error variables transients. To achieve a decoupling effect a feedback control law is needed together with a feed-forward regulator. The functional controllability represents a structural property of the system which must be proven. In this paper a decoupled and functional controller is obtained. The relevance of the motion functional controllability of the Robotino control is justified by the necessity of very fast and very precise loops of acceleration control counteracting errors in displacements caused by possible disturbance actions. In the past three decades, research on the geometric approach of dynamic systems theory and control has allowed this approach to become a powerful and a thorough tool for the analysis and synthesis of dynamic systems [1], [2], [3]. In [4], a robust decoupling controller using an algebraic state input feedback is presented, while this paper presents a robust decoupling controller using an algebraic output-input feedback. The goal of this paper is to propose a complete constructive procedure for the design of a decoupling controller. In Robotino case, to achieve a

decoupling between Horizontal, Vertical and Angular motions a preselecting field law is needed together with a feed-forward regulator. The paper is organised in the following way: Section

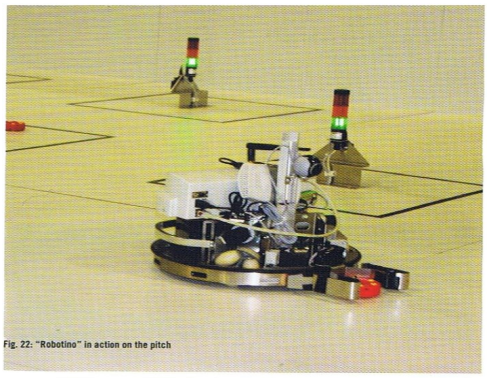

Figure 1. Robotino in action on the pitch.

2 presents a possible model of the Robotino. Section 3 shows the decoupling strategy using the geometric approach. Section 4 presents the functional controllability problem in the case of Robotino. At the end, numerical computer simulations, considering real data of the Robotino, are shown using Model Predictive Control (MPC), even though per sake of brevity this standard algorithm is not discussed.

2. Mechanical and Electrical Model Description

In Fig. 2 a diagram with the representation of the forces in the considered system is shown. If

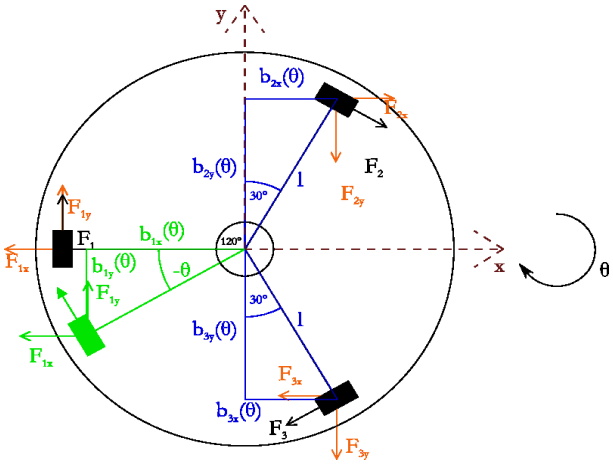

Figure 2. Mechanical schematic diagram of Robotino.

state vector $\mathbf{X}(t)$ is defined as, $x(t)$ and $y(t)$ positions of the center of mass of the system and its velocities, $\dot{x}(t)$ and $\dot{y}(t)$, moreover, considering the angular dynamics with its angular position $\theta(t)$ and its velocity $\dot{\theta}(t)$, then the following system is derived:

$$\begin{cases} \dot{\mathbf{X}}(t) = \mathbf{A}\mathbf{X}(t) + \mathbf{g}(\theta)\mathbf{F}(t) \\ \mathbf{O}(t) = \mathbf{C}\mathbf{X}(t), \end{cases} \tag{1}$$

with

$$\mathbf{X}(t) = \begin{bmatrix} x(t) \\ \dot{x}(t) \\ y(t) \\ \dot{y}(t) \\ \theta(t) \\ \dot{\theta}(t) \end{bmatrix}, \qquad \dot{\mathbf{X}}(t) = \begin{bmatrix} \dot{x}(t) \\ \ddot{x}(t) \\ \dot{y}(t) \\ \ddot{y}(t) \\ \dot{\theta}(t) \\ \ddot{\theta}(t), \end{bmatrix} \tag{2}$$

matrix

$$\mathbf{A} = \begin{bmatrix} 0 & 1 & 0 & 0 & 0 & 0 \\ 0 & -\frac{k_v}{M} & 0 & 0 & 0 & 0 \\ 0 & 0 & 0 & 1 & 0 & 0 \\ 0 & 0 & 0 & -\frac{k_v}{M} & 0 & 0 \\ 0 & 0 & 0 & 0 & 0 & 1 \\ 0 & 0 & 0 & 0 & 0 & -\frac{k_\theta}{J} \end{bmatrix}, \tag{3}$$

which for sake of notation can be written as follows:

$$\mathbf{A} = \begin{bmatrix} \mathbf{A}_{x2\times2} & \mathbf{0}_{2\times2} & \mathbf{0}_{2\times2} \\ \mathbf{0}_{2\times2} & \mathbf{A}_{y2\times2} & \mathbf{0}_{2\times2} \\ \mathbf{0}_{2\times2} & \mathbf{0}_{2\times2} & \mathbf{A}_{\theta2\times2} \end{bmatrix}, \tag{4}$$

where $\mathbf{A}_{x2\times2}$, $\mathbf{A}_{y2\times2}$ and $\mathbf{A}_{\theta2\times2}$ are the minor matrices of $\mathbf{A}$ describing the x, y and θ dynamics of the system. Matrix $\mathbf{C}$ represents the output matrix and can be written in the following way:

$$\mathbf{C} = \begin{bmatrix} 1 & 0 & 0 & 0 & 0 & 0 \\ 0 & 0 & 1 & 0 & 0 & 0 \\ 0 & 0 & 0 & 0 & 1 & 0 \end{bmatrix}, \tag{5}$$

where the following notation is assumed:

$$\mathbf{C_x} = \begin{bmatrix} 1 & 0 & 0 & 0 & 0 & 0 \end{bmatrix}, \tag{6}$$

$$\mathbf{C_y} = \begin{bmatrix} 0 & 0 & 1 & 0 & 0 & 0 \end{bmatrix}, \tag{7}$$

$$\mathbf{C}_\theta = \begin{bmatrix} 0 & 0 & 0 & 0 & 1 & 0 \end{bmatrix}. \tag{8}$$

Field $\mathbf{g}(\theta)$ is as follows:

$$\mathbf{g}(\theta) = \begin{bmatrix} 0 & 0 & 0 \\ \frac{\sin(\theta)}{M} & \frac{\sin(\frac{2}{3}\pi+\theta)}{M} & -\frac{\sin(\frac{2}{3}\pi-\theta)}{M} \\ 0 & 0 & 0 \\ \frac{\cos(\theta)}{M} & \frac{\cos(\frac{2}{3}\pi+\theta)}{M} & \frac{\cos(\frac{2}{3}\pi-\theta)}{M} \\ 0 & 0 & 0 \\ a & b & c \end{bmatrix} \tag{9}$$

where

$$a = \frac{\sin(\theta) \cdot l \cdot \sin(\theta) + \cos(\theta) \cdot l \cdot \cos(\theta)}{J},$$

$$b = \frac{\sin(\frac{2}{3}\pi + \theta) \cdot l \cdot \cos(\frac{\pi}{6} + \theta)}{J} + \frac{\cos(\frac{2}{3}\pi + \theta) \cdot l \cdot \sin(\frac{\pi}{6} + \theta)}{J} \tag{10}$$

and

$$c = \frac{-\sin(\frac{2}{3}\pi - \theta) \cdot l \cdot -\cos(\frac{\pi}{6} - \theta)}{J} + \frac{\cos(\frac{2}{3}\pi - \theta) \cdot l \cdot \sin(\frac{\pi}{6} - \theta)}{J} \tag{11}$$

and force input vector signal $\mathbf{F}(t) = \begin{bmatrix} F_1(t) \\ F_2(t) \\ F_3(t) \end{bmatrix}$ in which $F_1(t) = K_m i_1(t)/r$, $F_2(t) = K_m i_2(t)/r$ and $F_3(t) = K_m i_3(t)/r$, where K_m represents the motor constant, r the radius of the wheels and variables $i_1(t)$, $i_2(t)$ and $i_3(t)$ are the currents of the three DC-electrical drives. In fact, the Robotino consists of 3 DC electrical drives that power the three omniwheels. The models of these three DC-drives are reported below.

$$\begin{bmatrix} \frac{di_1(t)}{dt} \\ \frac{d\omega_1(t)}{dt} \\ \frac{di_2(t)}{dt} \\ \frac{d\omega_2(t)}{dt} \\ \frac{di_3(t)}{dt} \\ \frac{d\omega_3(t)}{dt} \end{bmatrix} = \begin{bmatrix} -\frac{R}{L} & -\frac{K_m}{L} & 0 & 0 & 0 & 0 \\ \frac{K_m}{J} & -\frac{K}{J} & 0 & 0 & 0 & 0 \\ 0 & 0 & -\frac{R}{L} & -\frac{K_m}{L} & 0 & 0 \\ 0 & 0 & \frac{K_m}{J} & -\frac{K}{J} & 0 & 0 \\ 0 & 0 & 0 & 0 & -\frac{R}{L} & -\frac{K_m}{L} \\ 0 & 0 & 0 & 0 & \frac{K_m}{J} & -\frac{K}{J} \end{bmatrix} \cdot \begin{bmatrix} i_1(t) \\ \omega_1(t) \\ i_2(t) \\ \omega_2(t) \\ i_3(t) \\ \omega_3(t) \end{bmatrix} + \begin{bmatrix} \frac{1}{L} & 0 & 0 \\ 0 & 0 & 0 \\ 0 & \frac{1}{L} & 0 \\ 0 & 0 & 0 \\ 0 & 0 & \frac{1}{L} \\ 0 & 0 & 0 \end{bmatrix} \cdot \begin{bmatrix} U_{inp_1}(t) \\ U_{inp_2}(t) \\ U_{inp_3}(t) \end{bmatrix}, \tag{12}$$

where $U_{inp_1}(t)$, $U_{inp_2}(t)$ and $U_{inp_3}(t)$ represent the input voltage of the DC-drive, L is the inductance, R is the resistance, J represents the motor inertia factor, K_m is the motor moment and finally K can be seen as the friction factor. This model is important in realising the simulation and is a basis for the inverted drive used in the control strategy.

3. Design of a Decoupling Controller

This section describes the design of a decoupling controller with respect to the x-y and θ motions above defined. A geometric approach is used in this analysis. Since the geometric relations depend on the rotational position (θ), the forces actuated by the three DC drives are needed to move in a certain direction and they may be difficult to be obtained.

Definition 1 *A control law for the dynamic system (1) is* decoupling *with respect to the regulated outputs $x(t)$, $y(t)$, and $\theta(t)$, if there exist partitions $F_x(t), F_y(t)$, and $F_\theta(t)$ of the input vector $\mathbf{F}(t)$ such that for zero initial conditions, each input $F_{(\cdot)}(t)$ (with all other inputs, identically zero) only affects the corresponding output $x(t)$, $y(t)$, or $\theta(t)$.* □

It it to be shown that there exists a decoupling and stabilizing state feedback field $\mathbf{D}(\theta)$, along with three input partition fields $\mathbf{T}_x(\theta)$, $\mathbf{T}_y(\theta)$, and $\mathbf{T}_\theta(\theta)$ such that, for the dynamic triples

$$\begin{array}{c} (\mathbf{C}_x,\, \mathbf{A} + \mathbf{g}(\theta)\mathbf{D}(\theta),\, \mathbf{g}(\theta)\mathbf{F}_1(t))\,, \\ (\mathbf{C}_y,\, \mathbf{A} + \mathbf{g}(\theta)\mathbf{D}(\theta),\, \mathbf{g}(\theta)\mathbf{F}_2)\,, \\ (\mathbf{C}_\theta,\, \mathbf{A} + \mathbf{g}(\theta)\mathbf{D}(\theta),\, \mathbf{g}(\theta)\mathbf{F}_3(t))\,, \end{array} \tag{13}$$

it holds the following conditions:

$$\mathcal{R}_x(\theta) = \mathsf{min}\mathcal{I}\Big(\mathbf{A} + \mathbf{g}(\theta)\mathbf{D}(\theta),\, \mathbf{g}(\theta)\mathbf{T}_x(\theta)\Big) \subseteq \mathcal{C}_y \cap \mathcal{C}_\theta \;\; \forall\theta, \tag{14}$$

and

$$\mathbf{C}_x\mathcal{R}_x(\theta) = \mathsf{im}(\mathbf{C}_x), \;\; \forall\theta. \tag{15}$$

$$\mathcal{R}_y(\theta) = \mathsf{min}\mathcal{I}\Big(\mathbf{A} + \mathbf{g}(\theta)\mathbf{D}(\theta),\, \mathbf{g}(\theta)\mathbf{T}_y(\theta)\Big) \subseteq \mathcal{C}_x \cap \mathcal{C}_\theta \;\; \forall\theta, \tag{16}$$

and

$$\mathbf{C}_y\mathcal{R}_y(\theta) = \mathsf{im}(\mathbf{C}_y), \;\; \forall\theta. \tag{17}$$

$$\mathcal{R}_\theta(\theta) = \mathsf{min}\mathcal{I}\Big(\mathbf{A} + \mathbf{g}(\theta)\mathbf{D}(\theta),\, \mathbf{g}(\theta)\mathbf{T}_\theta(\theta)\Big) \subseteq \mathcal{C}_x \cap \mathcal{C}_y \;\; \forall\theta, \tag{18}$$

and

$$\mathbf{C}_\theta\mathcal{R}_\theta(\theta) = \mathsf{im}(\mathbf{C}_\theta), \;\; \forall\theta. \tag{19}$$

Here,

$$\mathsf{min}\mathcal{I}(\mathbf{A}, \mathsf{im}(\mathbf{g}(\theta))) = \sum_{i=0}^{n-1} \mathbf{A}^i \mathsf{im}(\mathbf{g}(\theta))$$

is a minimum $\mathbf{A}$–invariant subspace containing $\mathsf{im}(\mathbf{g}(\theta))\ \forall\ \theta$. Moreover, the partition fields $\mathbf{T}_x(\theta)$, $\mathbf{T}_y(\theta)$ and $\mathbf{T}_\theta(\theta)$ satisfy the following relationships:

$$\begin{array}{l} \mathsf{im}(\mathbf{g}(\theta)\cdot\mathbf{T}_x(\theta)) = \mathsf{im}(\mathbf{g}(\theta)) \cap \mathcal{R}_x(\theta), \\ \mathsf{im}(\mathbf{g}(\theta)\cdot\mathbf{T}_y(\theta)) = \mathsf{im}(\mathbf{g}(\theta)) \cap \mathcal{R}_y(\theta), \\ \mathsf{im}(\mathbf{g}(\theta)\cdot\mathbf{T}_\theta(\theta)) = \mathsf{im}(\mathbf{g}(\theta)) \cap \mathcal{R}_\theta(\theta). \end{array} \tag{20}$$

The stabilizing field $\mathbf{D}(\theta)$ is such that:

$$(\mathbf{A} + \mathbf{g}(\theta)\mathbf{D}(\theta))\mathcal{R}_x(\theta) \subseteq \mathcal{R}_x(\theta), \tag{21}$$

$$(\mathbf{A} + \mathbf{g}(\theta)\mathbf{D}(\theta))\mathcal{R}_y(\theta) \subseteq \mathcal{R}_y(\theta), \tag{22}$$

and

$$(\mathbf{A} + \mathbf{g}(\theta)\mathbf{D}(\theta))\mathcal{R}_\theta(\theta) \subseteq \mathcal{R}_\theta(\theta). \tag{23}$$

Considering matrix $\mathbf{A}$ defined in (3) it is straightforward to see that this matrix is structurally already decoupled and intrinsically stable, this implies that field $\mathbf{D}(\theta) = \mathbf{0}\ \forall\theta$. Considering

$$\mathbf{T}(\theta) = [\mathbf{T}_x(\theta), \mathbf{T}_y(\theta), \mathbf{T}_\theta(\theta), \mathbf{T}_c(\theta)],$$

where $\mathbf{T}_c(\theta)$ is defined in a complementary fashion and it is straightforward to show that matrix $\mathbf{T}_c = \mathbf{0}$. In particular, matrix $\mathbf{T}_c$ represents the complementary field partition to the subspaces of x-position, y-position and angular position of the Robotino. The Robotino motion is described using just three variables, therefore partitions $\mathbf{T}_x(\theta), \mathbf{T}_y(\theta), \mathbf{T}_\theta(\theta)$ complete the transformation and thus $\mathbf{T}_c = \mathbf{0}$.

$$\mathsf{im}\mathbf{T}(\theta) = \mathsf{im}[\mathbf{T}_x(\theta), \mathbf{T}_y(\theta), \mathbf{T}_\theta(\theta)] = \mathsf{im}\mathbf{T}_x(\theta) \oplus \mathsf{im}\mathbf{T}_y(\theta) \oplus \mathsf{im}\mathbf{T}_\theta(\theta). \tag{24}$$

Considering the output matrices (6), (7) and (8) corresponding to x-position, y-position and angular position their respective kernels are as follows:

$$\mathcal{C}_x = \mathsf{im}\begin{bmatrix}0&0&0&0&0\\1&0&0&0&0\\0&1&0&0&0\\0&0&1&0&0\\0&0&0&1&0\\0&0&0&0&1\end{bmatrix},\quad \mathcal{C}_y = \mathsf{im}\begin{bmatrix}1&0&0&0&0\\0&-1&0&0&0\\0&0&0&0&0\\0&0&-1&0&0\\0&0&0&-1&0\\0&0&0&0&1\end{bmatrix},\quad \mathcal{C}_\theta = \mathsf{im}\begin{bmatrix}1&0&0&0&0\\0&1&0&0&0\\0&0&1&0&0\\0&0&0&-1&0\\0&0&0&0&0\\0&0&0&0&1\end{bmatrix}. \tag{25}$$

According to relation (9) it is straightforward to observe that the following three equations hold $\forall\ \theta$;

$$\mathsf{im}(\mathbf{g}(\theta)) \cap \big(\mathcal{C}_x \cap \mathcal{C}_y\big) \neq \mathbf{0}, \tag{26}$$

$$\mathsf{im}(\mathbf{g}(\theta)) \cap \big(\mathcal{C}_x \cap \mathcal{C}_\theta\big) \neq \mathbf{0}, \tag{27}$$

$$\mathsf{im}(\mathbf{g}(\theta)) \cap \big(\mathcal{C}_y) \cap \mathcal{C}_\theta\big) \neq \mathbf{0}. \tag{28}$$

Field $\mathbf{g}(\theta)$ is a function of θ without singularities if $\theta \neq \pi/2 + k\pi$ with $k \in \mathbb{N}$. For sake of brevity the following field is calculated considering just $\theta = 0$:

$$(\mathbf{g}(\theta))^\dagger = \begin{bmatrix}0&0&0&a(\theta)&0&b(\theta)\\0&c(\theta)&0&-a(\theta)&0&b(\theta)\\0&-c(\theta)&0&-a(\theta)&0&b(\theta)\end{bmatrix}, \tag{29}$$

where with $(\mathbf{g}(\theta))^\dagger$ the pseudo inverse of field $\mathbf{g}(\theta)$ is indicated. Functions $a(\theta)$, $b(\theta)$ and $c(\theta)$ are functions of the variable θ with $\theta \approx 0$. The following calculation is obtained for $\theta \neq \pi/2 + k\pi$ with $k \in \mathbb{N}$:

$$\mathcal{C}_x \cap \mathcal{C}_y = \mathsf{im}\begin{bmatrix}0&0&0&0\\1&0&0&0\\0&0&0&0\\0&-1&0&0\\0&0&-1&0\\0&0&0&1\end{bmatrix},\quad \mathcal{C}_\theta \cap \mathcal{C}_y = \mathsf{im}\begin{bmatrix}1&0&0&0\\0&1&0&0\\0&0&0&0\\0&0&1&0\\0&0&0&0\\0&0&0&1\end{bmatrix},\quad \mathcal{C}_\theta \cap \mathcal{C}x = \mathsf{im}\begin{bmatrix}0&0&0&0\\1&0&0&0\\0&1&0&0\\0&0&1&0\\0&0&0&0\\0&0&0&1\end{bmatrix}. \tag{30}$$

The following calculation allows to get the required fields for the decoupling of the mechanical system:

$$\mathbf{T}_\theta(\theta) = (\mathbf{g}(\theta))^\dagger \cdot \mathsf{im}(\mathbf{g}(\theta)) \cap \mathcal{C}_x \cap \mathcal{C}_y, \tag{31}$$

$$\mathbf{T}_x(\theta) = (\mathbf{g}(\theta))^\dagger \cdot \mathsf{im}(\mathbf{g}(\theta)) \cap \mathcal{C}_\theta \cap \mathcal{C}_y, \tag{32}$$

$$\mathbf{T}_y(\theta) = (\mathbf{g}(\theta))^\dagger \cdot \mathsf{im}(\mathbf{g}(\theta)) \cap \mathcal{C}_\theta) \cap \mathcal{C}_x. \tag{33}$$

Adding all 3 T-Fields together, we get a new field $\mathbf{T}(\theta)$:

$$\mathbf{T}(\theta) = \mathbf{T}_x(\theta) + \mathbf{T}_y(\theta) + \mathbf{T}_\theta(\theta). \tag{34}$$

Field $\mathbf{T}(\theta)$ can be seen as a preselecting field and the following product realises the mechanical decoupling:

$$\mathcal{B} = \mathsf{im}(\mathbf{g}(\theta)\mathbf{T}(\theta)) = \mathsf{im}\begin{bmatrix}0&0&0\\1&0&0\\0&0&0\\0&1&0\\0&0&0\\0&0&1\end{bmatrix}, \tag{35}$$

in which matrix $\mathbf{B}$ can be seen as a resulting input matrix.

4. On the Functional Controllability of the Robotino

This section is aimed to the analysis of the output functional controllability of the Robotino system. As already pointed out, we are interested in controlling motion tracking without transients of error variables. In the whole, in the Robotino control, the exact trajectory tracking is an ambitious objective and this is particularly emphasized by advanced control tasks recalled in Section 1. For solving the problem, the natural approach is to analyze the constrained output controllability idea, [5] and [1], formalized below.

Definition 2 (Perfect output controllability) *Given the triple* $(\mathbf{A}, \mathbf{B}, \mathbf{C})$*, the output subspace* $\mathcal{L}^i$ *is said to be perfect output functionally controllable with respect to i-th derivative and with respect to the subspace of states* $\mathcal{F}$ *if* $\mathcal{L}^i = \mathbf{C}\mathcal{F}$ *and, for every initial state* $\mathbf{x}_0 \in \mathcal{F}$*, it is possible, by means of proper bounded and measurable control functions, to follow in* $\mathcal{L}$ *any trajectory arbitrarily given in the class of functions which admit i-th derivative with respect to time, while the state evolves into* $\mathcal{F}$*.*

□

Recall, cf. [5], that the output functional controllability is strictly related to the geometric–type extension of the relative degree for multivariable systems and that each subspace $\mathcal{F}$ satisfying Definition 2 is $(\mathbf{A}, \mathbf{B})$–controlled invariant.
The following theorem which was demonstrated in [5] and in [1] is reported here below to be applied for the Robotino case.

Theorem 1 *(***Output Functional Controllability and Decoupling of the Robotino***) The output subspaces* $\mathsf{im}(\mathbf{C}_x)$*,* $\mathsf{im}(\mathbf{C}_y)$ *and* $\mathsf{im}(\mathbf{C}_\theta)$ *are output functionally controllable with respect to the* 3^{rd} *derivative and with respect to the constrained reachable subspaces* $\mathcal{R}_x(\theta)$*,* $\mathcal{R}_y(\theta)$*, and* $\mathcal{R}_\theta(\theta)$ *respectively. Moreover, field* $\mathbf{T}(\theta)$ *makes the system, with outputs* $x(t)$*,* $y(t)$ *and* $\theta(t)$ *decoupled and output functionally controllable.*

□

Remark 1 *Regarding the functional controllability of rigid body as object motions, the* 3^{rd} *order of derivative means that the outputs* $x(t)$*,* $y(t)$ *and* $\theta(t)$ *can perfectly track any desired trajectories* $x_d(t)$*,* $y_d(t)$ *and* $\theta_d(t)$ *which has a piecewise continuous* 3^{rd} *derivative. This is true for all initial states* $\mathbf{x}_o$ *in* $\mathcal{R}_x(\theta)$*,* $\mathcal{R}_y(\theta)$*, and* $\mathcal{R}_\theta(\theta)$ *and with piecewise continuous control functions* $\mathbf{F}(t)$*. Furthermore, it could be easily shown that order* 3 *of the rigid body object motions is not due to the particular choice of the subspaces* $\mathcal{R}_x(\theta)$*,* $\mathcal{R}_y(\theta)$*, and* $\mathcal{R}_\theta(\theta)$ *but it is an inherent property of the system. It is related to the relative degree of the relationship between the rigid body object motion and the DC-Drive input voltage.*

□

In the following a fundamental condition is shown, further details in [5].

Projection Condition
Given the system represented as $(\mathbf{A}, \mathbf{B}, \mathbf{C})$*.* $\mathcal{F}^i$ *is a subspace of functional controllability of the output with respect to the i-derivative, if and only if:*

$$\mathcal{F}^i \subseteq \mathcal{F}^i \cap \mathcal{Z}_{i-1} + \mathcal{C}, \tag{36}$$

where $\mathcal{Z}^{i-1}$ *is defined in the following way:* $\mathcal{Z}_o = \mathcal{B}$ *and* $\mathcal{Z}_j = \mathcal{B} + \mathbf{A}(\mathcal{Z}_{j-1} \cap \mathcal{F}^i \cap \mathcal{C})$*.* □

Sketch of the proof considering the Robotino case

It is to be remarked that the Projection Condition states a necessary and sufficient condition for functional controllability of a system. If just the mechanical part of the model is considered, it is possible to show that an output controllability with respect to the second derivative is obtained. In fact, in case $i = 2$, in a generic point $\overline{\mathbf{x}} \in \mathcal{F}^2$ of a generic trajectory, exists, per definition, at least a velocity of state $\dot{\overline{\mathbf{x}}} \in \mathcal{F}^2$. All admissible velocities on $\mathcal{F}^2$ are obtained adding to $\dot{\overline{\mathbf{x}}}$ vectors belonging to subspace $\mathcal{F}^2 \cap \mathcal{B}$. Thus, such a subspace represents the set of all possible velocity variations and $\mathcal{F}^2 \cap \mathcal{B} \cap \mathcal{C}$ represents the set of all velocity variations which are not visible from the output. Being in general

$$\ddot{\mathbf{x}}(t) = \mathbf{A}\dot{\mathbf{x}}(t) + \mathbf{B}\dot{\mathbf{u}}(t), \tag{37}$$

then with a suitable choice of the control $u_1(t)+u_2(t)$, in which $u_1(t)$ is manipulable in its second derivative and such that $\mathbf{B}u_1(t) \in \mathcal{F}^2 \cap \mathcal{B} \cap \mathcal{C}$, and $u_2(t)$ is manipulable in its first derivative and such that $\mathbf{B}u_2(t) \in \mathcal{B}$. Thus, if the trajectory evolves in the following subspace

$$\mathcal{Z}_1 = \mathcal{B} + \mathbf{A}\mathcal{F}^2 \cap \mathcal{B} \cap \mathcal{C}, \tag{38}$$

it is possible to variate the second derivative of it. A trajectory belongs to $\mathcal{F}^2$ if its derivative belongs to $\mathcal{F}^2$ (invariant subspace definition according to [1]) and it is necessary that its variations belong to $\mathcal{Z}_1 \cap \mathcal{F}^2$. If $\mathcal{L}^2$ indicates an output subspace, then $\mathcal{L}^2 = \mathbf{C}\mathcal{F}^2$ is a subspace of output functional controllability with respect to the second derivative if and only if:

$$\mathbf{C}\mathcal{F}^2 = \mathbf{C}(\mathcal{F}^2 \cap \mathcal{Z}_1), \tag{39}$$

or

$$\mathcal{F}^2 + \mathcal{C} = \mathbf{C}(\mathcal{F}^2 \cap \mathcal{Z}_1) + \mathcal{C}. \tag{40}$$

□

Remark 2 *In other words, subspace $\mathcal{Z}_1$ represents the subspace of all the manipulable trajectories with continuous second derivative. If the trajectory belongs to $\mathcal{Z}_1$, then it is possible to manipulate the first and the second derivatives in $\mathcal{Z}_1$. This can be done by means of proper bounded and measurable control functions. In fact in so doing, it is possible to follow in $\mathcal{L}^2$ any trajectory arbitrarily given in the class of functions which admit 2^{nd} derivative with respect to time, while the state evolves into $\mathcal{F}^2$.*

□

Considering again the mechanical system and choosing subspaces $\mathcal{F}_x$, $\mathcal{F}_y$ and $\mathcal{F}_\theta$ as candidate subspaces:

$$\mathcal{F}_x = \mathsf{im}\begin{bmatrix} 1 & 0 \\ 0 & 1 \\ 0 & 0 \\ 0 & 0 \\ 0 & 0 \\ 0 & 0 \end{bmatrix}, \qquad \mathcal{F}_y = \mathsf{im}\begin{bmatrix} 0 & 0 \\ 0 & 0 \\ 1 & 0 \\ 0 & 1 \\ 0 & 0 \\ 0 & 0 \end{bmatrix}, \qquad \text{and} \quad \mathcal{F}_\theta = \mathsf{im}\begin{bmatrix} 0 & 0 \\ 0 & 0 \\ 0 & 0 \\ 0 & 0 \\ 1 & 0 \\ 0 & 1 \end{bmatrix}. \tag{41}$$

It can be shown that the mechanical system with this choice of subspaces can be functionally controllable on trajectories with continuous 2^{nd} derivatives. In fact, considering that $\mathcal{F}^1 \nsubseteq \mathcal{F}^1 \cap \mathcal{Z}_0 + \mathcal{C}_x$, to be more precise

$$\mathcal{F}_x^1 \cap \mathcal{Z}_0 = \begin{bmatrix} 0 \\ 1 \\ 0 \\ 0 \\ 0 \\ 0 \end{bmatrix}, \tag{42}$$

so the mechanical system is not functionally controllable with respect to trajectories of the 1^{st} order. Similar results can be obtained for considering the output subspace $\mathsf{im}\mathbf{C}_y$ and $\mathsf{im}\mathbf{C}_\theta$. If the following relation is considered $\mathcal{F}_x^2 \subseteq \mathcal{F}_x^2 \cap \mathcal{Z}_1 + \mathcal{C}_x$, to be more precise

$$\mathcal{Z}_1 = \begin{bmatrix} 0 & 0 & 0 \\ 1 & 0 & 0 \\ 0 & 0 & 0 \\ 0 & 1 & 0 \\ 0 & 0 & 0 \\ 0 & 0 & 1 \end{bmatrix} + \begin{bmatrix} 0 & 1 & 0 & 0 & 0 & 0 \\ 0 & -\frac{k_v}{M} & 0 & 0 & 0 & 0 \\ 0 & 0 & 0 & 1 & 0 & 0 \\ 0 & 0 & 0 & -\frac{k_v}{M} & 0 & 0 \\ 0 & 0 & 0 & 0 & 0 & 1 \\ 0 & 0 & 0 & 0 & 0 & -\frac{k_\theta}{J} \end{bmatrix}.$$

$$\mathsf{im}\begin{bmatrix} 1 & 0 \\ 0 & 1 \\ 0 & 0 \\ 0 & 0 \\ 0 & 0 \\ 0 & 0 \end{bmatrix} \cap \begin{bmatrix} 0 & 0 & 0 \\ 1 & 0 & 0 \\ 0 & 0 & 0 \\ 0 & 1 & 0 \\ 0 & 0 & 0 \\ 0 & 0 & 1 \end{bmatrix} \cap \mathsf{im}\begin{bmatrix} 0 & 0 & 0 \\ 1 & 0 & 0 \\ 0 & 0 & 0 \\ 0 & -1 & 0 \\ 0 & 0 & 0 \\ 0 & 0 & 1 \end{bmatrix} = \mathcal{B}. \quad (43)$$

$$\mathcal{F}_x^2 \cap \mathcal{Z}_1 = \mathcal{F}_x^2. \quad (44)$$

It is possible to see then that equation (39) is satisfied thus also equation (40) is satisfied. Similar results can be obtained after considering the output subspace $\mathsf{im}\mathbf{C}_y$ and $\mathsf{im}\mathbf{C}_\theta$.

Remark 3 *After considering relation (40) it is possible to see that functional subspace $\mathcal{F}^2$ consists of the position subspace along trajectory x(t) and its velocity subspace. Moreover, the velocity subspace belongs to $\mathcal{C}_x$. Similar considerations can be obtained considering the output subspace $\mathsf{im}\mathbf{C}_y$ and $\mathsf{im}\mathbf{C}_\theta$.* □

Considering the electrical drive which is connected in input to the mechanical drive, it can be shown that this system is functionally controllable considering trajectories with continuous 1^{st} derivative. To conclude, considering the cascade structure of the whole system, the Robotino can be functionally controlled considering trajectories with continuous 3^{rd} derivative.

5. Simulation Results

Figure 3 shows the Simulink/Matlab block diagram used for simulation. Using a decentralized MPC-controller with the geometric decoupling approach acting as a pre-control, different trajectories can be tracked. As such the MPC accepts trajectories in horizontal, vertical and angular direction and attempts to direct the Robotino only in the specified direction. For sake of brevity the control strategy is not presented. Therefore, it is possible to move the Robotino along the x-axis without a rotation for example.

Figure 4 shows a very accurate movements along the desired trajectory which is represented in the tested case by a circle and by an avoidance trajectory path. In Fig. 5 the current in case of the circle and the avoidance trajectory are represented. The circle is realized considering a continuous sine and a cosine function on the X and Y movements. These signals are visible in term of voltages of the X and Y drives in Fig. 6. It is possible to observe from Fig. 6 that the cosine function is not exactly reproducible because its not continuity function and this effect is also visible in the left part of Fig. 4 in which a considerable initial error occurs. Additionally it is vital, that the drives are not forced to output more than they can handle, so voltages and currents would have to remain in their respective boundaries. The right part of Fig. 4 shows a possible trajectory avoidance which is a typical requirement in the Robotino tasks. From

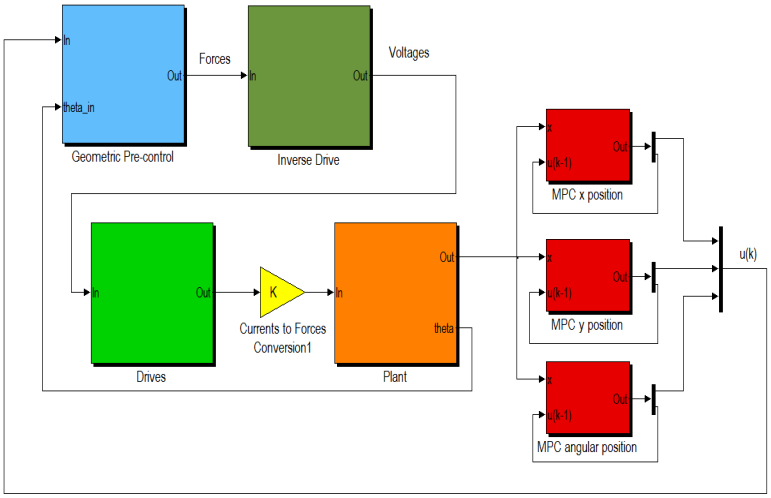

Figure 3. Block diagram of the control system structure

the right part of Fig. 4 it is possible to see an initial error in the trajectory tracking. This is a structural error due, as before, to the desired trajectory function which is a function of $\mathcal{C}^0$ (continuous function). Nevertheless, if the initial error represented in the left part of Fig. 4 is compared with that of the right part, it is possible to remark that in the case of obstacle avoidance the error seems to be smaller than that in the circle case. This aspect can be justified considering that the X Y movement generating functions in the case of obstacle avoidance are a sine and a ramp, so they are continuous functions. Figure 5 shows in term of currents those two different loads. In particular, the case of obstacle avoidance presents a lower level of currents in the transient phase.

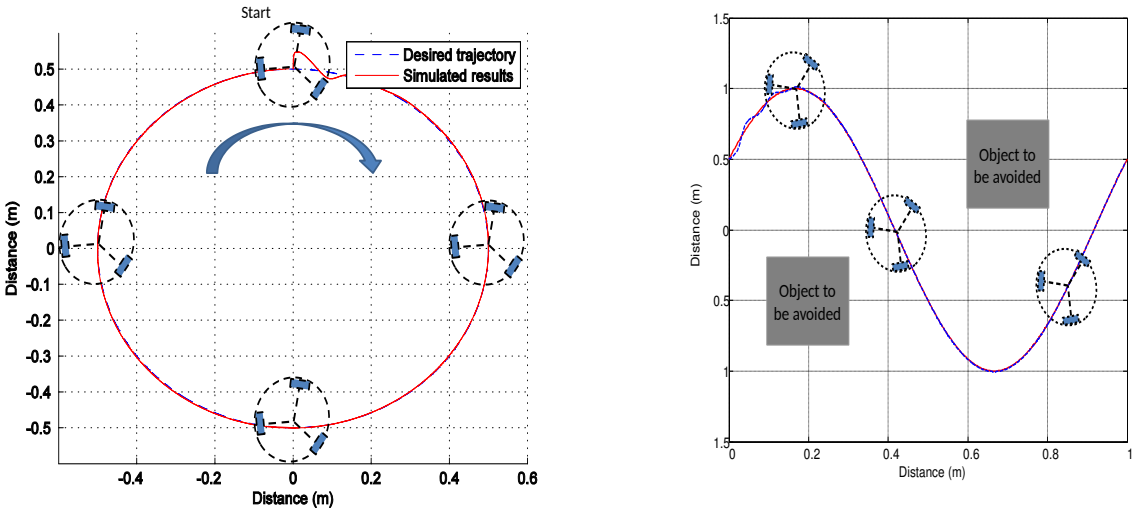

Figure 4. X-Y-Trajectory of the Robotino (left). Trajectory object avoidance (right)

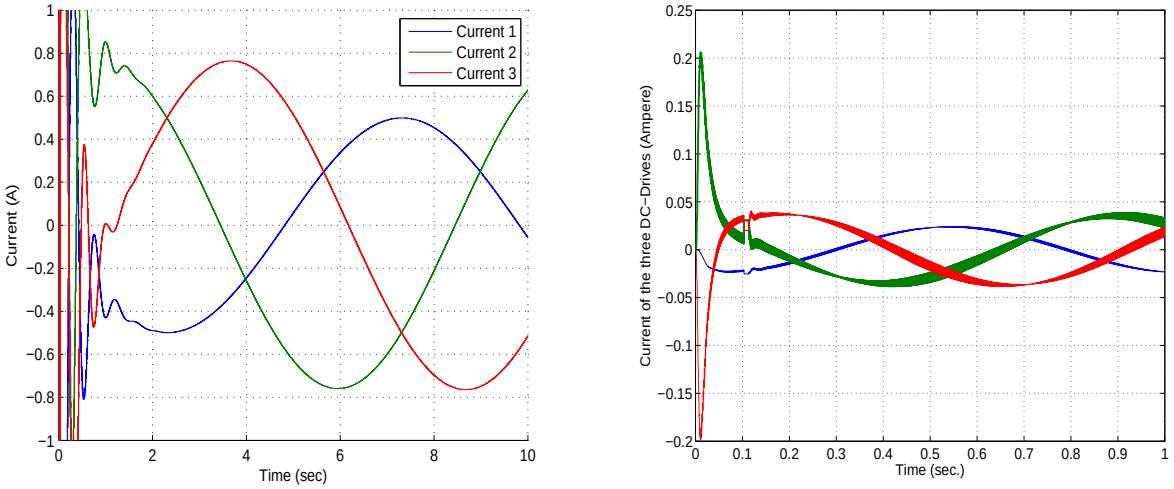

Figure 5. Currents of the three drives acting the three wheels in the case of trajectory avoidance (left). Currents of the three drives acting the three wheels in the case of trajectory avoidance (right)

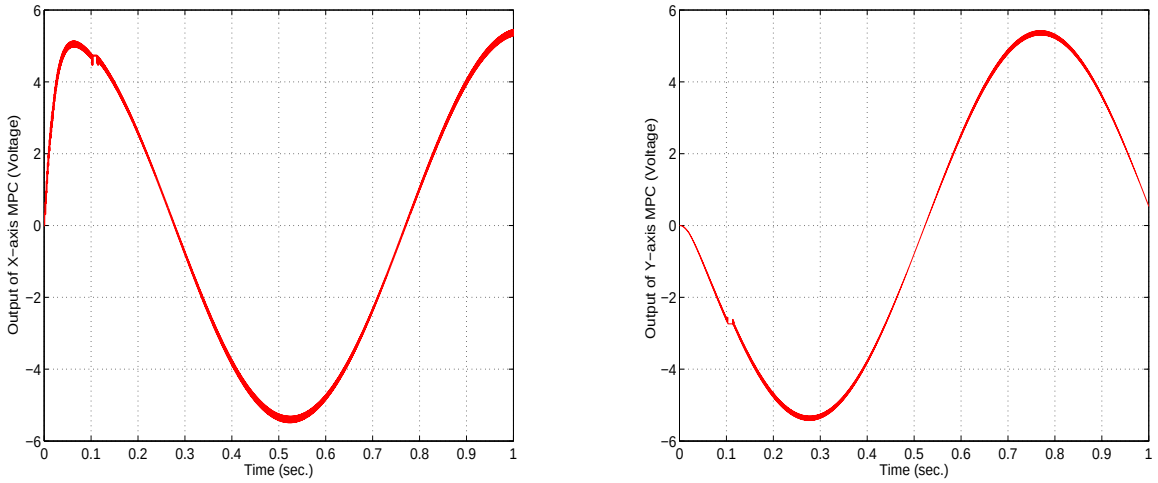

Figure 6. Output of X-axis and Y-axis MPC

6. Conclusion

This paper presents a procedure in order to obtain the decoupling functional controllability between horizontal, vertical and angular motions using an geometric approach. Here, the functional decoupling problem is investigated. To achieve a decoupling effect a feedback control law is needed together with a feed-forward regulator. The relevance of the motion functional controllability in the Robotino control is justified by the necessity of very fast and very precise loops of acceleration control counteracting errors in displacements caused by possible disturbance actions. Simulation results are shown to indicate the potential of this approach.

References

[1] G. Basile and G. Marro. *Controlled and conditioned invariants in linear system theory.* Prentice Hall, New Jersey, 1992.
[2] A. Isidori. *Nonlinear control Systems: an introduction.* Springer, Berlin, 1989.
[3] W.M. Wonham. *Linear multivariable control: a geometric approach.* Springer, New York, 1979.
[4] P. Mercorelli and D. Prattichizzo. A geometric procedure for robust decoupling control of contact forces in robotic manipulation. *Kybernetika*, 39(4):433–455, 2003.
[5] G. Basile and G. Marro. A state space approach to non-interacting controls. *Ricerche di Automatica*, 1(1):68–77, 1970.